Electronic Supplementary Material (ESI) for Journal of Materials Chemistry A.
This journal is © The Royal Society of Chemistry 2016

Electronic Supplementary Information (ESI)

Photon Energy Storage Materials with High Energy Densities Based on Diacetylene-Azobenzene Derivatives

Ggoch Ddeul Han, Sarah Sunah Park, Yun Liu, David Zhitomirsky, Eugene Cho, Mircea Dincă, and Jeffrey C. Grossman*

Synthesis of azobenzene-functionalized diacetylenes (monomers) ^{1}H and ^{13}C NMR spectra are shown in Fig. S11.

Compound **1**. To a solution of dodeca-5,7-diynedioic acid (490 mg, 2.2 mmol) in dichloromethane (50 mL), oxalyl chloride (567 µL, 6.6 mmol) was added dropwise at room temperature and stirred for 10 min. Catalytic amount (a drop) of dimethylformamide was added to the mixture, and the solution was stirred overnight generating CO_2 (g), CO (g), and HCl (g) through a bubbler. The reaction mixture was dried under reduced pressure (50 mTorr) for 2 h to obtain dodeca-5,7-diynedioyl dichloride (light brown oil) which was used for the next step without further purification. The dichloride (356 mg, 1.37 mmol) was dissolved in dry THF (2 mL) which was added dropwise to the mixture of 4-phenylazoaniline (813 mg, 4.12 mmol) and triethylamine (1.7 mL, 12.4 mmol) in dichloromethane (50 mL). After the gas evolution stopped, the mixture was stirred overnight, and the resulting precipitate was filtered, rinsed with dichloromethane, and dried under reduced pressure. The light yellow powder product (621.1 mg) was obtained with 78.1 % yield. mp 266 °C; ^{1}H NMR (500 MHz, DMF-d_7, δ): 10.50 (s, 2H; N-H), 7.95 (m, 12H; Ar H), 7.61 (m, 6H; Ar H), 2.60 (t, 4H; CH_2), 2.47 (t, 4H; CH_2), 1.90 (m, 4H; CH_2); ^{13}C NMR (500 MHz, DMF-d_7, δ): 172.17 (C=O), 153.49 (Ar), 148.88 (Ar), 143.90 (Ar), 131.89 (Ar), 130.32 (Ar, C–H), 124.67 (Ar, C–H), 123.40 (Ar, C–H), 120.24 (Ar, C–H), 78.23

(C≡C), 66.61 (C≡C), 36.38 (CH_2), 24.92 (CH_2), 19.09 (CH_2); HRMS (ESI) *m*/*z*: $[M + H]^+$ calcd for $C_{36}H_{32}N_6O_2$, 581.2660; found, 581.2640.; Anal. Calcd for $C_{36}H_{32}N_6O_2$: C, 74.46; H, 5.55; N, 14.47%. Found: C, 74.23; H, 5.57; N, 14.29%.

Compound **2**. To a solution of hexadeca-7,9-diynedioic acid (170 mg, 0.61 mmol) in dichloromethane (50 mL), oxalyl chloride (157 µL, 1.83 mmol) was added dropwise at room temperature and stirred for 10 min. Catalytic amount (a drop) of dimethylformamide was added to the mixture, and the solution was stirred overnight generating CO_2 (g), CO (g), and HCl (g) through a bubbler. The reaction mixture was dried under reduced pressure (50 mTorr) for 2 h to obtain hexadeca-7,9-diynedioyl dichloride (light yellow oil) which was used for the next step without further purification. The dichloride (192.3 mg, 0.61 mmol) was dissolved in dry THF (2 mL) which was added dropwise to the mixture of 4-phenylazoaniline (361 mg, 1.83 mmol) and triethylamine (765 µL, 5.49 mmol) in dichloromethane (50 mL). After the gas evolution stopped, the mixture was stirred overnight, and the resulting precipitate was filtered, rinsed with dichloromethane, and dried under reduced pressure. The light yellow powder product (321.9 mg) was obtained with 82.9 % yield. mp 233 °C; ^{1}H NMR (500 MHz, DMF-d_7, δ): 10.41 (s, 2H; N-H), 7.95 (m, 12H; Ar H), 7.62 (m, 6H; Ar H), 2.46 (t, 4H; CH_2), 2.35 (t, 4H; CH_2), 1.70 (m, 4H; CH_2), 1.55 (m, 4H; CH_2), 1.46 (m, 4H; CH_2); ^{13}C NMR (500 MHz, DMF-d_7, δ): 172.82 (C=O), 153.49 (Ar), 148.84 (Ar), 143.98 (Ar), 131.89 (Ar), 130.32 (Ar, C–H), 124.68 (Ar, C–H), 123.38 (Ar, C–H), 120.18 (Ar, C–H), 78.60 (C≡C), 66.27 (C≡C), 37.59 (CH_2), 29.21 (CH_2), 28.93 (CH_2), 25.74 (CH_2), 19.32 (CH_2); HRMS (ESI) *m*/*z*: $[M + Na]^+$ calcd for $C_{40}H_{40}N_6O_2$, 659.3105; found, 659.3109.; Anal. Calcd for $C_{40}H_{40}N_6O_2$: C, 75.45; H, 6.33; N, 13.20%. Found: C, 75.19; H, 6.16; N, 13.04%.

Compound **3**. To a solution of docosa-10,12-diynedioic acid (310 mg, 0.86 mmol) in dichloromethane (50 mL), oxalyl chloride (220 µL, 2.6 mmol) was added dropwise at room temperature and stirred for 10 min. Catalytic amount (a drop) of dimethylformamide was added to the mixture, and the solution was stirred overnight generating CO_2 (g), CO (g), and HCl (g) through a bubbler. The reaction mixture was dried under reduced pressure (50 mTorr) for 2 h to obtain docosa-10,12-diynedioyl dichloride (light yellow oil) which was used for the next step without further purification. The dichloride (343 mg, 0.86 mmol) was dissolved in dry THF (2 mL) which was added dropwise to the mixture of 4-phenylazoaniline (509 mg, 2.58 mmol) and triethylamine (1.1 mL, 7.7 mmol) in dichloromethane (50 mL). After the gas evolution stopped, the mixture was stirred overnight, and the resulting precipitate was filtered, rinsed with dichloromethane, and dried under reduced pressure. The light yellow powder product (456.6 mg) was obtained with 73.6 % yield. mp 213 °C; ^{1}H NMR (500 MHz, DMF-d_7, δ): 10.37 (s, 2H; N-H), 7.95 (m, 12H; Ar H), 7.61 (m, 6H; Ar H), 2.45 (t, 4H; CH_2), 2.32 (t, 4H; CH_2), 1.69 (m, 4H; CH_2), 1.49 (m, 4H; CH_2), 1.32 (m, 16H; CH_2); ^{13}C NMR (500 MHz, DMF-d_7, δ): 173.37 (C=O), 153.88 (Ar), 149.20 (Ar), 144.41 (Ar), 132.26 (Ar, C–H), 130.70 (Ar, C–H), 125.06 (Ar, C–H), 123.76 (Ar, C–H), 120.53 (Ar, C–H), 79.06 (C≡C), 66.61 (C≡C), 38.15 (CH_2), 30.35 (CH_2), 30.24 (CH_2), 30.10 (CH_2), 29.96 (CH_2), 29.48 (CH_2), 26.65 (CH_2), 19.76 (CH_2); HRMS (ESI) *m*/*z*: $[M + Na]^+$ calcd for $C_{46}H_{52}N_6O_2$, 743.4044; found, 743.4044.; Anal. Calcd for $C_{46}H_{52}N_6O_2$: C, 76.63; H, 7.27; N, 11.66%. Found: C, 76.49; H, 7.16; N, 11.49%.

Compound **4**. The docosa-10,12-diynedioyl dichloride (166 mg, 0.42 mmol) was dissolved in dry THF (2 mL) which was added dropwise to the mixture of 4-phenylazophenol (248 mg, 1.25 mmol) and triethylamine (522 µL, 3.75 mmol) in dichloromethane (50 mL). After the gas evolution stopped, the mixture was stirred overnight. The clear yellow solution was dried under reduced pressure to leave orange powder which was dispersed and sonicated in the mixture of dichloromethane (3 mL) and hexane (15 mL). The resulting precipitate was filtered, rinsed with dichloromethane/hexane, and dried under reduced pressure. The yellow powder was re-dissolved in dichloromethane (20 mL), extracted with H_2O three times, dried over $MgSO_4$, cooled in an ice bath, and filtered to remove impurity (white salt). The filtrate was dried under reduced pressure. The light yellow powder product (216.7 mg) was obtained with 72.1 % yield. mp 136 °C; ^{1}H NMR (500 MHz, CD_2Cl_2, δ): 7.99 (m, 4H; Ar H), 7.93 (m, 4H; Ar H), 7.56 (m, 6H; Ar H), 7.28 (d, 4H; Ar H), 2.61 (t, 4H; CH_2), 2.27 (t, 4H; CH_2), 1.77 (m, 4H; CH_2), 1.40 (m, 20H; CH_2); ^{13}C NMR (500 MHz, CD_2Cl_2, δ): 172.62 (C=O), 153.64 (Ar), 153.21 (Ar), 150.82 (Ar), 131.80 (Ar, C–H), 129.81 (Ar, C–H), 124.60 (Ar, C–H), 123.45 (Ar, C–H), 123.07 (Ar, C–H), 78.23 (C≡C), 65.78 (C≡C), 34.96 (CH_2), 29.78 (CH_2), 29.68 (CH_2), 29.58 (CH_2), 29.46 (CH_2), 29.05 (CH_2), 25.49 (CH_2), 19.76 (CH_2); HRMS (ESI) *m*/*z*: $[M + H]^+$ calcd for $C_{46}H_{50}N_4O_4$, 723.3905; found, 723.4007.; Anal. Calcd for $C_{46}H_{50}N_4O_4$: C, 76.43; H, 6.97; N, 7.75%. Found: C, 76.16; H, 6.80; N, 7.71%.

Compound **5**. The docosa-10,12-diynedioyl dichloride (166 mg, 0.42 mmol) was dissolved in dry THF (2 mL) which was added dropwise to the mixture of *N*,*N*-dimethyl-4,4’-azodianiline (300 mg, 1.25 mmol) and triethylamine (522 µL, 3.75 mmol) in dichloromethane (50 mL). After the gas evolution stopped, the mixture was stirred overnight, and the resulting precipitate was filtered, rinsed with dichloromethane, and dried under reduced pressure. The light yellow-brown powder product (253.0 mg) was obtained with 75.4 % yield.; ^{1}H NMR (500 MHz, DMF-d_7, δ): 10.25 (s, 2H; N-H), 7.88 (d, 4H; Ar H), 7.82 (m, 8H; Ar H), 6.89 (d, 4H; Ar H), 3.10 (s, 12H; CH_3), 2.43 (t, 4H; CH_2), 2.32 (t, 4H; CH_2), 1.68 (m, 4H; CH_2), 1.50 (m, 4H; CH_2), 1.32 (m, 16H; CH_2); ^{13}C NMR (500 MHz, DMF-d_7, δ): 172.77 (C=O), 153.47 (Ar), 149.35 (Ar), 144.18 (Ar), 142.45 (Ar), 125.36 (Ar, C–H), 123.60 (Ar, C–H), 120.17 (Ar, C–H), 112.55 (Ar, C–H), 78.69 (C≡C), 66.24 (C≡C), 40.47 (CH_3), 37.74 (CH_2), 30.06 (CH_2), 30.00 (CH_2), 29.73 (CH_2), 29.58

(CH_2), 29.11 (CH_2), 26.36 (CH_2), 19.38 (CH_2); HRMS (ESI) *m*/*z*: $[M + H]^+$ calcd for $C_{50}H_{62}N_8O_2$, 807.5068; found, 807.5069.

Compound **6**. The docosa-10,12-diynedioyl dichloride (166 mg, 0.42 mmol) was dissolved in dry THF (2 mL) which was added dropwise to the solution of Disperse black 9 (375 mg, 1.25 mmol) in dichloromethane/THF (50 mL). The mixture was stirred at 60 ^oC overnight, and the resulting dark blue material was hydrolyzed by Na_2CO_3 (aq). The mixture was extracted with H_2O, and the precipitate in organic layer was filtered, rinsed with dichloromethane and acetone, and dried under reduced pressure. The orange powder product (216.4 mg) was obtained with 56.1 % yield.; ^1H NMR (500 MHz, DMF-*d*$_7$, δ): 10.22 (s, 2H; N-H), 7.87 (d, 4H; Ar H), 7.80 (m, 8H; Ar H), 6.94 (d, 4H; Ar H), 3.76 (t, 8H; CH_2), 3.67 (t, 8H; CH_2), 2.42 (t, 4H; CH_2), 2.32 (t, 4H; CH_2), 1.68 (m, 4H; CH_2), 1.50 (m, 4H; CH_2), 1.32 (m, 16H; CH_2); ^{13}C NMR (500 MHz, DMF-*d*$_7$, δ): 172.69 (C=O), 151.88 (Ar), 149.46 (Ar), 143.90 (Ar), 142.21 (Ar), 125.52 (Ar, C–H), 123.58 (Ar, C–H), 120.16 (Ar, C–H), 112.39 (Ar, C–H), 78.69 (C≡C), 66.25 (C≡C), 59.85 (CH_2), 54.80 (CH_2), 37.76 (CH_2), 30.06 (CH_2), 30.00 (CH_2), 29.74 (CH_2), 29.59 (CH_2), 29.12 (CH_2), 26.34 (CH_2), 19.40 (CH_2); HRMS (ESI) *m*/*z*: $[M + H]^+$ calcd for $C_{54}H_{70}N_8O_6$, 927.5494; found, 927.5509.

Compound **7**. The docosa-10,12-diynedioyl dichloride (166 mg, 0.42 mmol) was dissolved in dry THF (2 mL) which was added dropwise to the mixture of Disperse orange 3 (303 mg, 1.25 mmol) and triethylamine (522 µL, 3.75 mmol) in dichloromethane (50 mL). After the gas evolution stopped, the mixture was stirred overnight, and the resulting precipitate was filtered, rinsed with dichloromethane, and dried under reduced pressure. The brown powder product (110.5 mg) was obtained with 32.8 % yield.; ^1H NMR (500 MHz, DMF-*d*$_7$, δ): 10.71 (s, 2H; N-H), 8.50 (d, 4H; Ar H), 8.13 (d, 4H; Ar H), 8.02 (m, 8H; Ar H), 2.49 (t, 4H; CH_2), 2.32 (t, 4H;

CH_2), 1.69 (m, 4H; CH_2), 1.50 (m, 4H; CH_2), 1.32 (m, 16H; CH_2); ^{13}C NMR (500 MHz, DMF-*d*$_7$, δ): 173.31 (C=O), 156.84 (Ar), 149.40 (Ar), 148.78 (Ar), 145.42 (Ar, C–H), 125.98 (Ar, C–H), 125.50 (Ar, C–H), 124.25 (Ar, C–H), 120.23 (Ar, C–H), 78.69 (C≡C), 66.25 (C≡C), 37.78 (CH_2), 30.04 (CH_2), 29.97 (CH_2), 29.73 (CH_2), 29.57 (CH_2), 29.10 (CH_2), 26.26 (CH_2), 19.39 (CH_2); HRMS (ESI) *m*/*z*: $[M + H]^+$ calcd for $C_{46}H_{50}N_8O_6$, 811.3926; found, 811.3903.

Compound **8**. The docosa-10,12-diynedioyl dichloride (166 mg, 0.42 mmol) was dissolved in dry THF (2 mL) which was added dropwise to the mixture of Disperse orange 13 (440 mg, 1.25 mmol) and triethylamine (522 µL, 3.75 mmol) in dichloromethane (50 mL). After the gas evolution stopped, the mixture was stirred overnight. The dark red solution was mixed with hexane (150 mL), and the resulting precipitate was filtered, rinsed with dichloromethane/hexane (1:2) and acetone, then dried under reduced pressure. The red powder product (400.6 mg) was obtained with 93.5 % yield.; ^1H NMR (500 MHz, CD_2Cl_2, δ): 9.06 (m, 4H; Ar H), 8.14 (m, 10H; Ar H), 7.81 (m, 4H; Ar H), 7.62 (m, 8H; Ar H), 7.34 (d, 4H; Ar H), 2.63 (t, 4H; CH_2), 2.28 (t, 4H; CH_2), 1.79 (m, 4H; CH_2), 1.43 (m, 20H; CH_2); ^{13}C NMR (500 MHz, CD_2Cl_2, δ): 172.60 (C=O), 154.02 (Ar), 153.97 (Ar), 151.53 (Ar), 149.67 (Ar), 149.58 (Ar), 132.89 (Ar), 132.24 (Ar), 129.95 (Ar, C–H), 128.05 (Ar, C–H), 125.14 (Ar, C–H), 124.26 (Ar, C–H), 123.23 (Ar, C–H), 124.01 (Ar, C–H), 123.22 (Ar, C–H), 112.90 (Ar, C–H), 112.86 (Ar, C–H), 78.25 (C≡C), 65.81 (C≡C), 34.99 (CH_2), 29.79 (CH_2), 29.69 (CH_2), 29.59 (CH_2), 29.47 (CH_2), 29.06 (CH_2), 25.50 (CH_2), 19.78 (CH_2); HRMS (ESI) *m*/*z*: $[M + H]^+$ calcd for $C_{66}H_{62}N_8O_4$, 1031.4967; found, 1031.4961.

Synthesis of polydiacetylenes via photopolymerization of diacetylene monomers

Diacetylene monomers were dispersed and sonicated in a solvent (dichloromethane or dichloromethane/hexane) without much dissolution, then dropcast onto a glass substrate to form a non-transparent thick film. A UV lamp (254 nm, 4 W) was placed 3–4 cm above the diacetylene film over several minutes depending on the rate of photopolymerization of each monomer. The films typically turn from light yellow to blue or purple, indicating the formation of polydiacetylenes. Then the polymer films were scraped off from the substrate and re-dispersed in a solvent to dropcast a new film, if the content of monomer was visually significant. The process of photopolymerization was repeated until the color of monomer disappeared.

Fig. S1. Azobenzene-functionalized diacetylenes with various terminal functional groups.

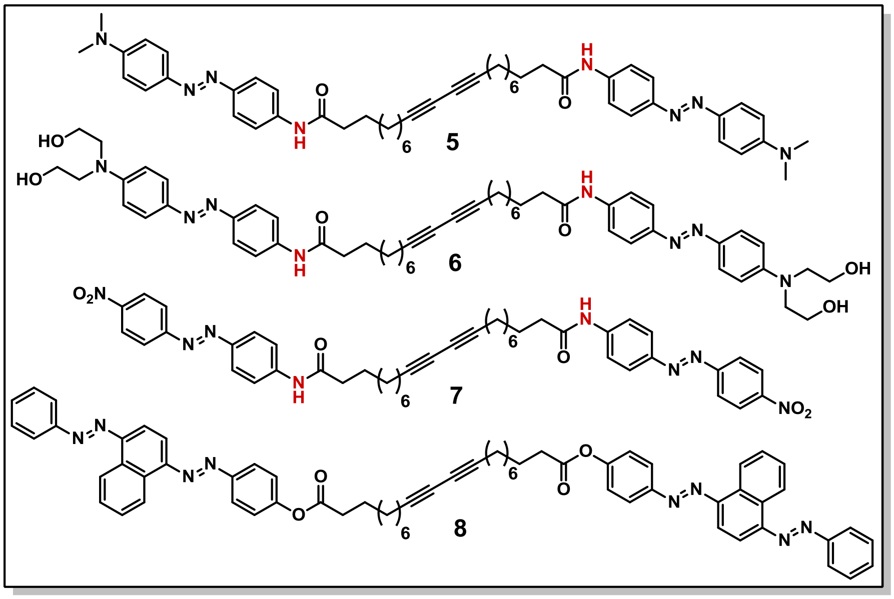

Compound **5–8** are docosa-10,12-diynes that are amide- or ester-linked to azobenenes functionalized with terminal groups. Compound **5** and **6** both incorporate electron-donating amino groups, and particularly compound **6** has alcohol groups for additional H-bonding capability. Compound **7** has electron-withdrawing nitro groups while compound **8** includes 1,4-bis(phenyldiazenyl)naphthalene groups which lead to greater volume change over isomerization compared to azobenzene groups. Tailoring electron density and delocalization on azo groups affects their optical properties such as HOMO–LUMO gap and π–π*/n–π* transitions which determine the chargeability of photon energy storage materials.

Fig. S2. (a) Molecular packing of compound **3** shown along *a* axis. C=O and N-H groups are staggered, hence intermolecular H-bonding is absent along this direction. Red, gray, blue and white spheres represent O, C, N and H atoms, respectively. H atoms omitted for clarity. (b) PXRD patterns of compound **3** compared to that simulated for single crystals.

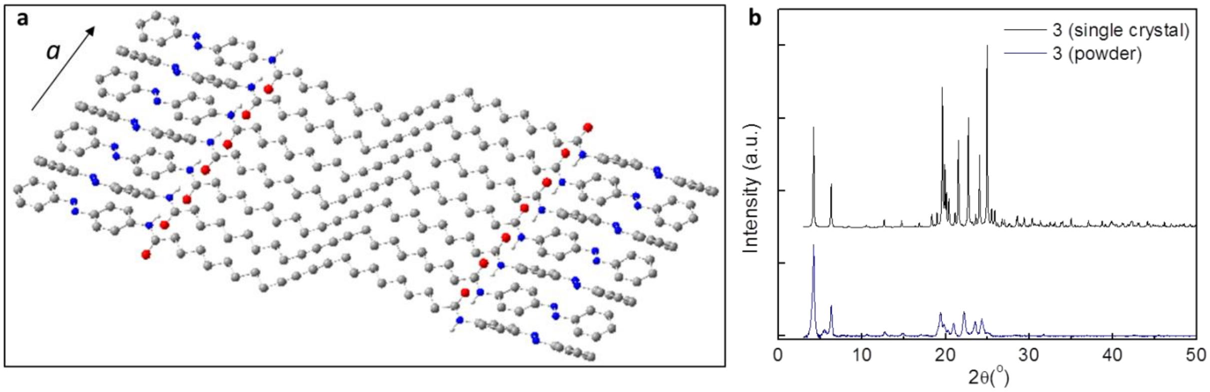

Fig. S3. A structure of polymer **3** optimized from *ab initio* simulations where side chains are packed along *b* axis. Blue, red, light blue, and white spheres correspond to N, O, C, and H atoms, respectively. Silver shade around the atoms represents the charge density iso-surface at the value of 0.1 e $Å^{-3}$. As observed from the overlapping of the charge density iso-surface, no hydrogen bonding exists between the amide groups

.

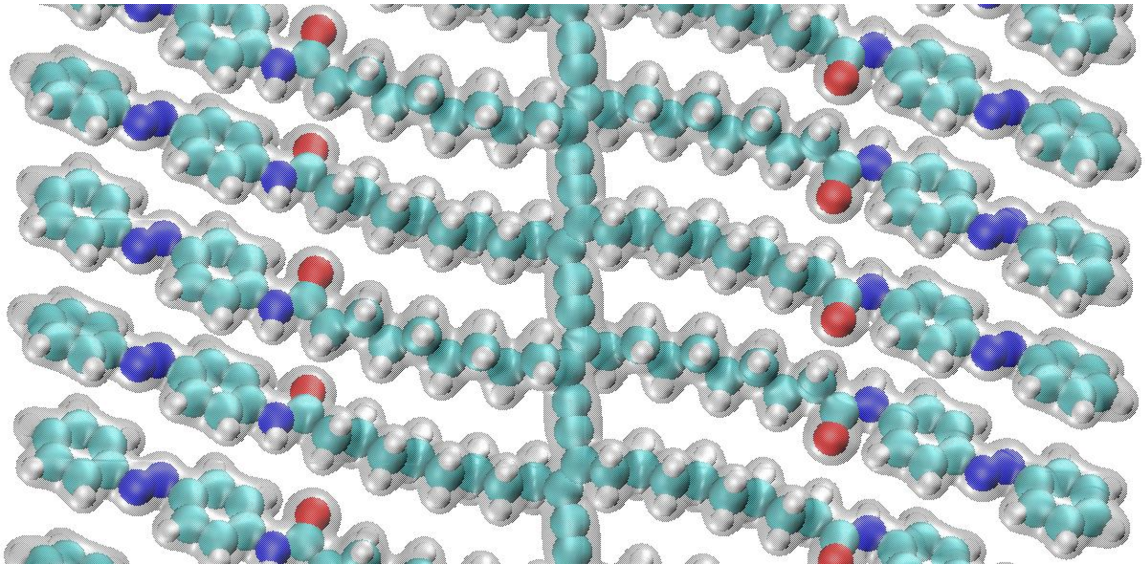

Fig. S4. Reversible thermochromism of polymer **3** films observed by variable-temperature UV–Vis absorption spectroscopy while heating up to 200 °C and cooling down to room temperatures. Inset shows the photographs of the films that change the color reversibly.

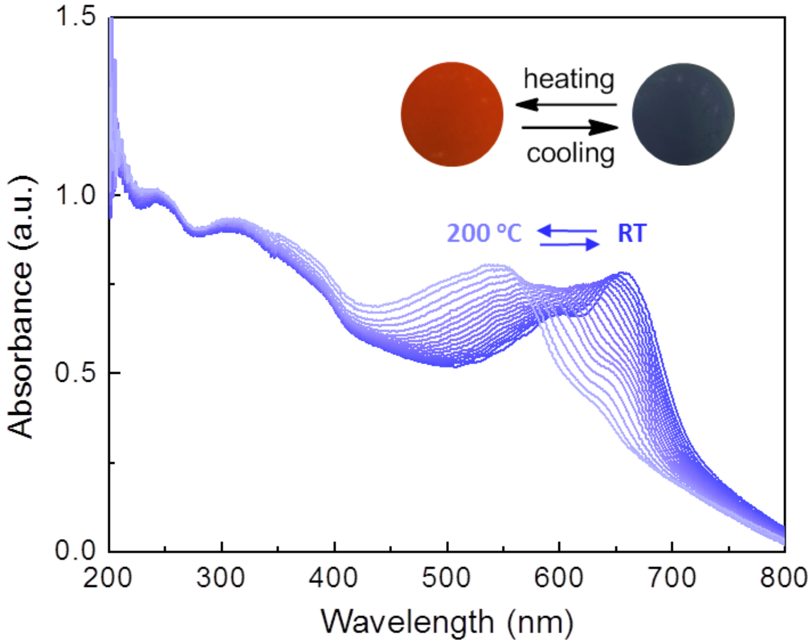

Fig. S5. UV-Vis absorption spectra of compound **1-8** in 10 μg mL^{-1} solution of DMF (a,b,c,e,f,g) or DCM (d,h).

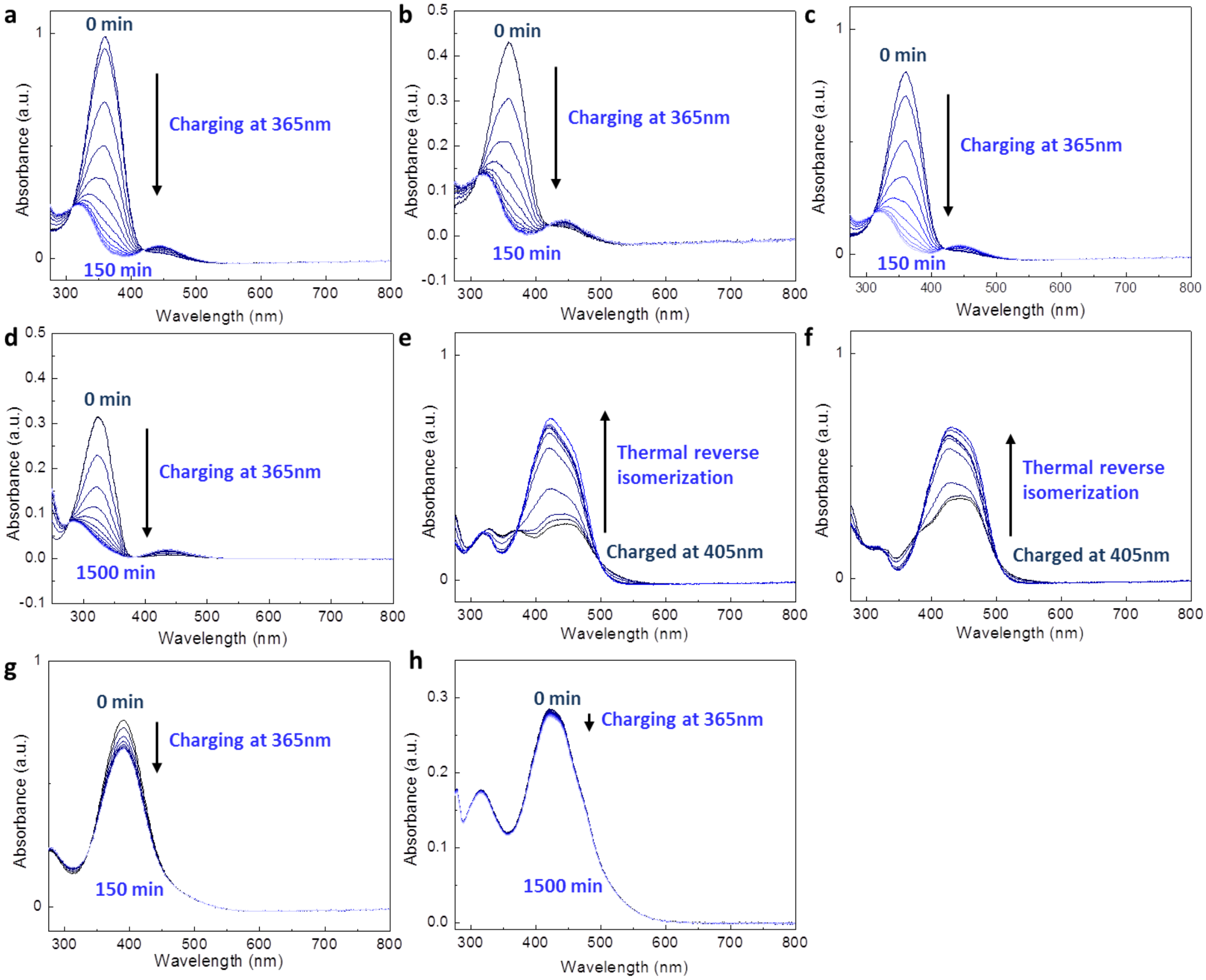

For compound **5–6** with terminal amino groups, light absorption feature is broadened and red-shifted to a range of 350–500 nm (e–f). Therefore, the compounds reach equilibrium of charging–discharging under ambient light, and are discharged rapidly in dark. Irradiation at 360 nm only decreases the overall intensity of the absorption peak without changing its shape. However, two distinguished peaks around 390 nm and 460 nm appear when the compounds are illuminated at 405 nm, as a result of more selectively excited π–π* transition. Compound **7** with terminal nitro groups also exhibits single peak centered at 390 nm, and charging it at either 365 nm or 405 nm decreases its intensity only slightly due to the large overlap between π–π* and n–π* transitions (g). Compound **8** displays the most red-shifted absorption spectra ranging from 350 nm to 600 nm, attributed to its extended π-system, and charging it at either 365 nm or 405 nm is the least efficient among the series of compounds (h). Heat release of monomer **5–8** was negligible, so is not discussed in this report.

Fig. S6. DSC analysis of charged compound **1** heated and cooled at 5 ^{o}C min^{-1} for two consecutive cycles.

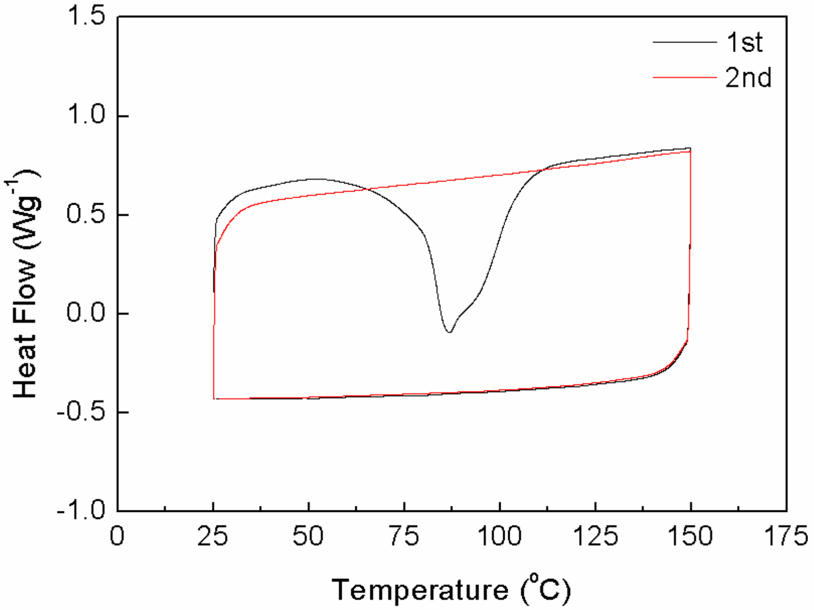

The heating of charged *cis* molecules results in the thermal reversion to *trans* isomers which do not exhibit endothermic or exothermic behaviors. The identical phenomenon is observed for the other compounds (**2–4**) within the relative temperature range.

Kinetic studies on thermal reverse isomerization and $t_{0.5}$ of compound 3–4.

Fig. S7 (a). Eyring-Polanyi plot (R^2 = 0.99997) for the thermal *cis→trans* isomerization of compound **3** in DMF. $\Delta H^{\ddagger}$= 88.74 kJ/mol; $\Delta S^{\ddagger}$= −45.82 kJ/mol; $t_{0.5}$ = 1.16 d (27.8 h).

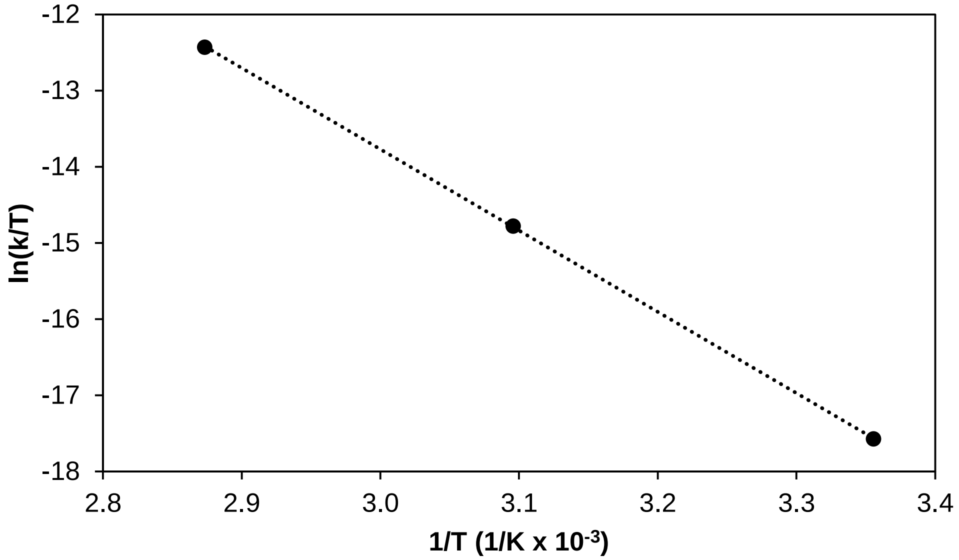

Fig. S7 (b). Eyring-Polanyi plot (R^2 = 0.99998) for the thermal *cis→trans* isomerization of compound **4** in DMF. $\Delta H^{\ddagger}$= 88.70 kJ/mol; $\Delta S^{\ddagger}$= −56.58 kJ/mol; $t_{0.5}$ = 4.10 d (98.4 h).

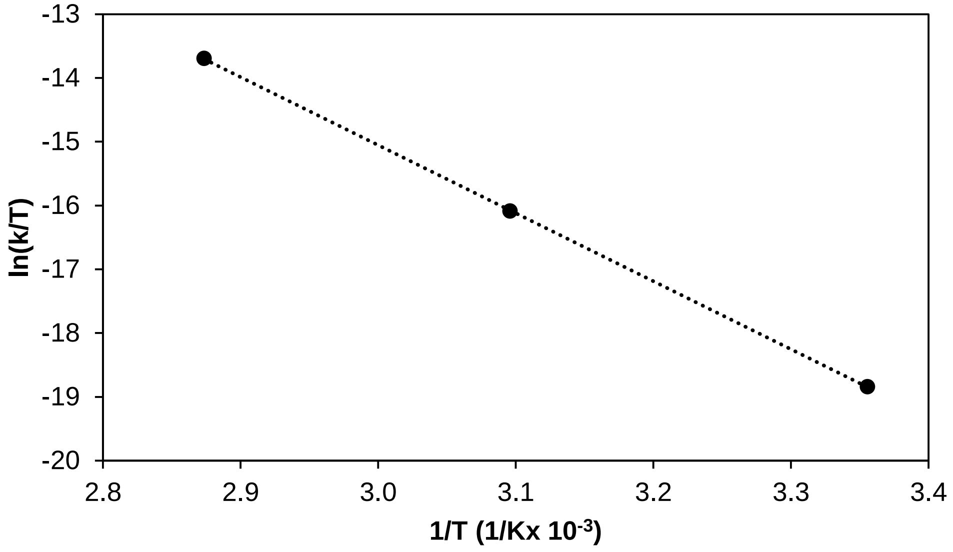

Solutions of compound **3** (92.8 µM) and **4** (79.1µM) in DMF were individually irradiated with 365 nm light while recording absorption spectra over time until the photostationary state was generated. They were then placed in dark and heated to the desired temperatures (25 ºC, 50 ºC, and 75 ºC), and the spectra were recorded over time to monitor the thermal reverse isomerization process. The solutions were vigorously stirred at all times.

The absorbance vs. time over the range of 342 nm to 352 nm at 1 nm increment were fit to the following formula. The obtained first order rate constant k is the average over this range.

$$\Delta OD = a(1 - be^{-kt})$$

The Eyring – Polanyi analysis follows the following equation

$$\ln\frac{k}{T} = -\frac{\Delta H^{\ddagger}}{R}\frac{1}{T} + \ln\frac{k_B}{h} + \frac{\Delta S^{\ddagger}}{R}$$

where k is the rate constant, T is the temperature, R is the gas constant, $k_B$is the Boltzmann constant, h is the Plank's constant, $\Delta H^{\ddagger}$is the enthalpy of activation, and $\Delta S^{\ddagger}$ is the entropy of activation.

The half-life at 25ºC was computed directly using the rate constant extracted from absorbance vs. time spectra at 25ºC.

$$t_{0.5} = \frac{\ln 2}{k}$$

Table S1. Rate constants of compound **3** and **4** at respective temperatures.

Compound	k×10^6 (sec^{-1}) at 25 ºC	50 ºC	75 ºC
3	6.94	123.16	1390.84
4	1.96	33.28	391.76

Fig. S8. (a-d) PXRD of monomer **1-4** as synthesized (*trans*), charged (*cis*), discharged (*trans*), and melt-crystalized (*trans*). (e) PXRD of monomer **5-8** as synthesized (*trans*).

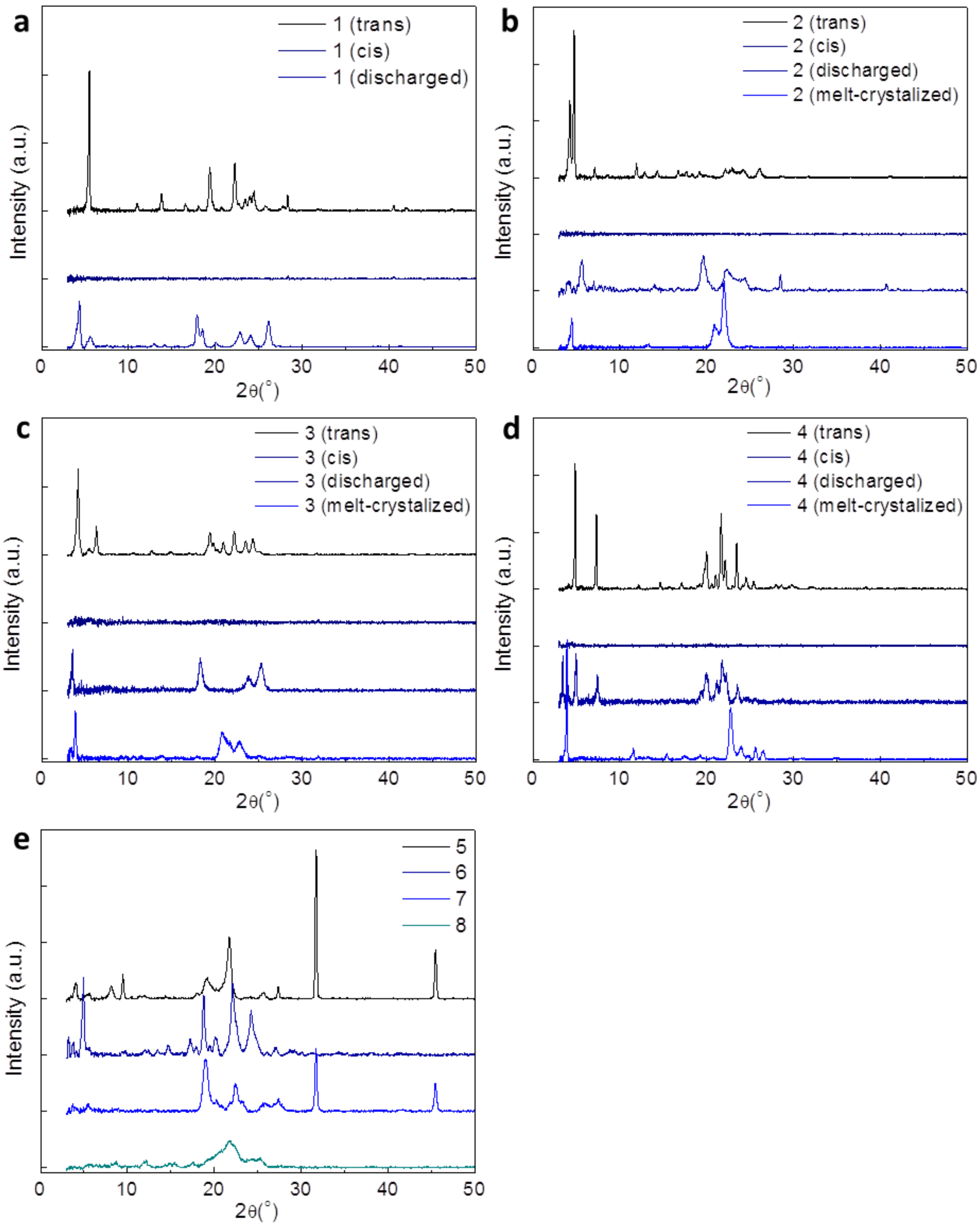

In order to gauge how similar the isomerization-assisted phase transition from amorphous or liquid state to crystalline solid state is compared to the traditional liquid-to-solid phase transition, PXRD of compound **2**–**4** were also taken after melt-crystallization by DSC. The melt-crystallized solid exhibits different diffraction patterns from those of the discharged compounds often with enhanced crystallinity. Compound **1** was decomposed during melting, so melt-crystallization was not accomplished.

Fig. S9. (a-d) PXRD of polymer **1-4** as synthesized (trans), charged (cis), discharged (trans), and melt-crystalized (trans).

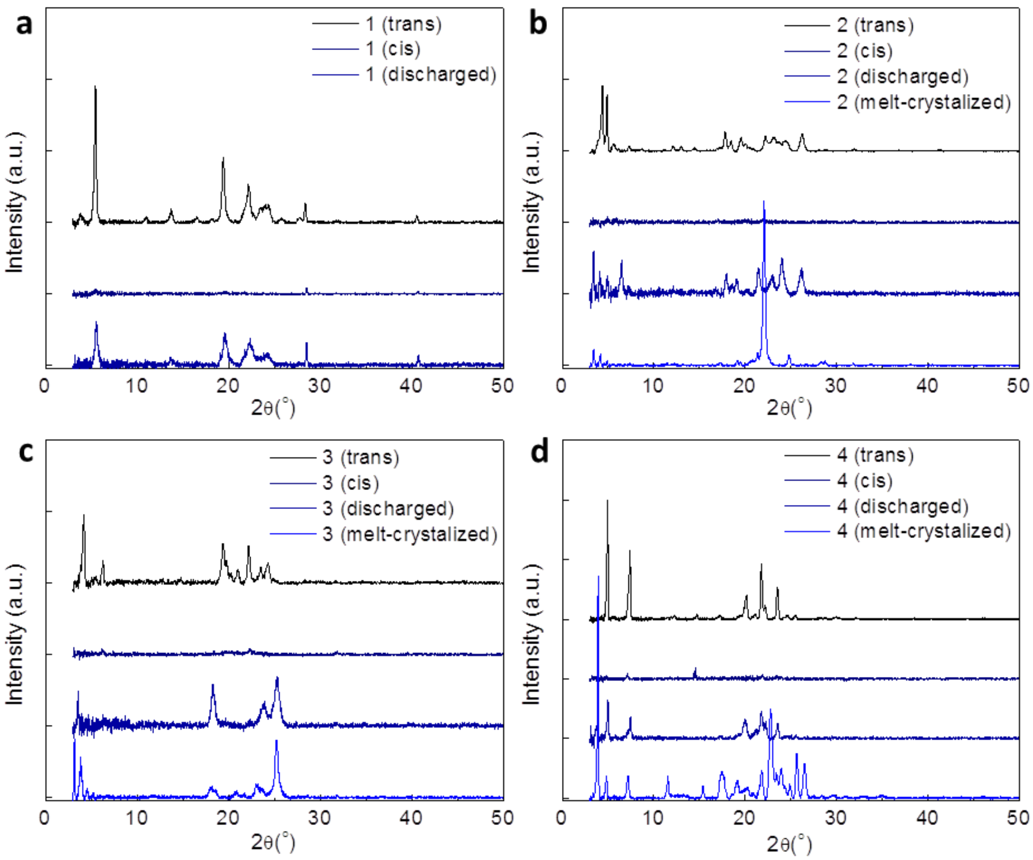

Fig. S10. Thermogravimetric analysis (TGA) plots for monomer **1-4**. Decomposition temperatures range from 260 ^{o}C to 290 ^{o}C. Heating was conducted from 50 ^{o}C to 800 ^{o}C at a rate of 20 ^{o}C min^{-1}.

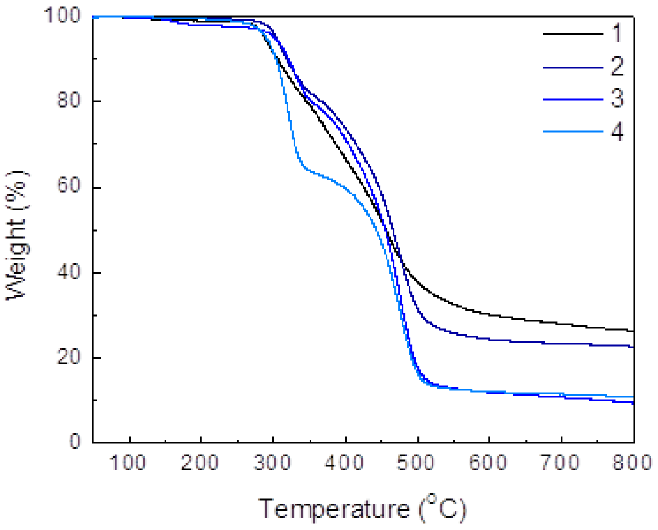

Fig. S11. ^{1}H and ^{13}C NMR spectra of compound **1** (a,b), **2** (c,d), **3** (e,f), **4** (g,h), **5** (i,j), **6** (k,l), **7** (m,n), and **8** (o,p).

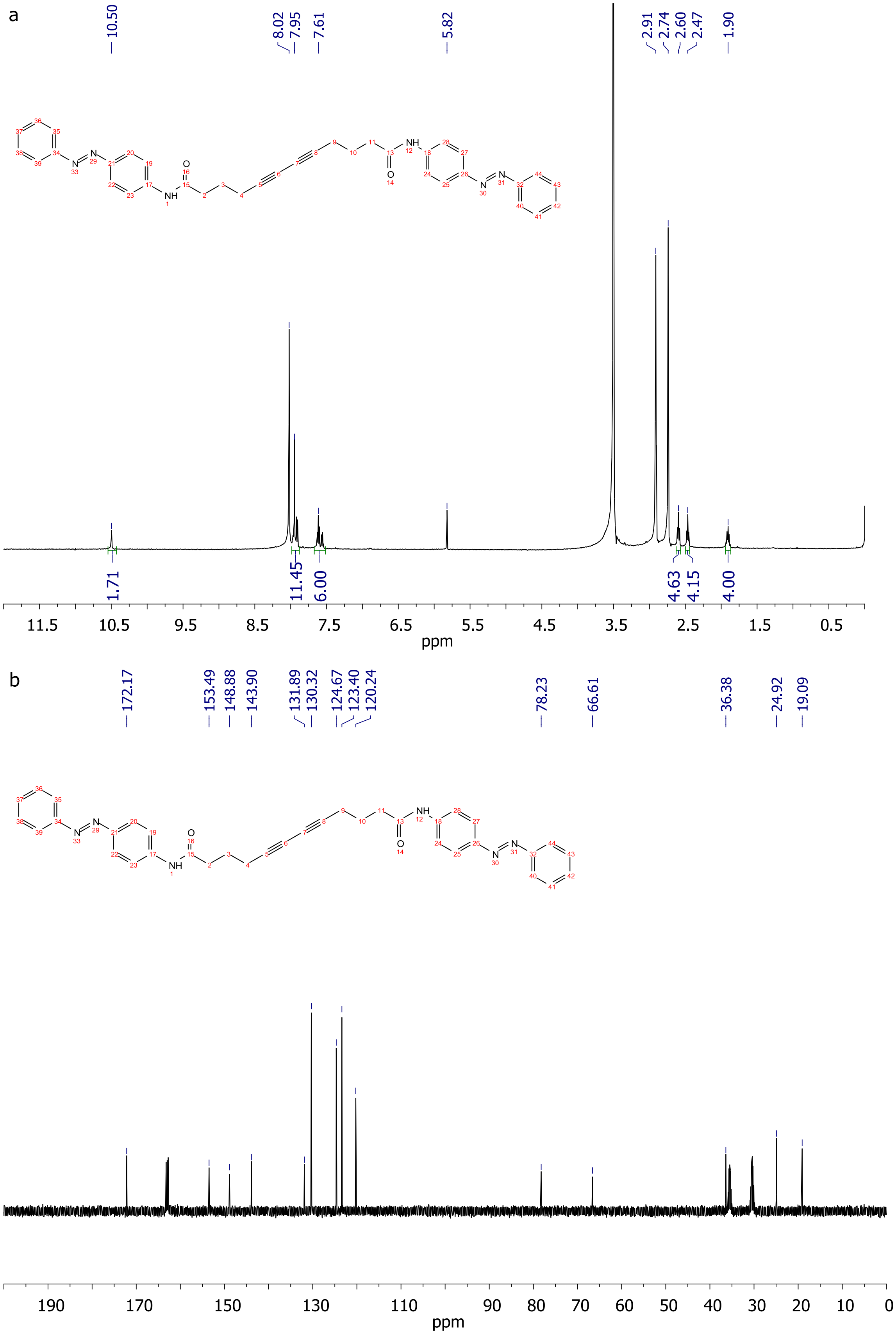

c

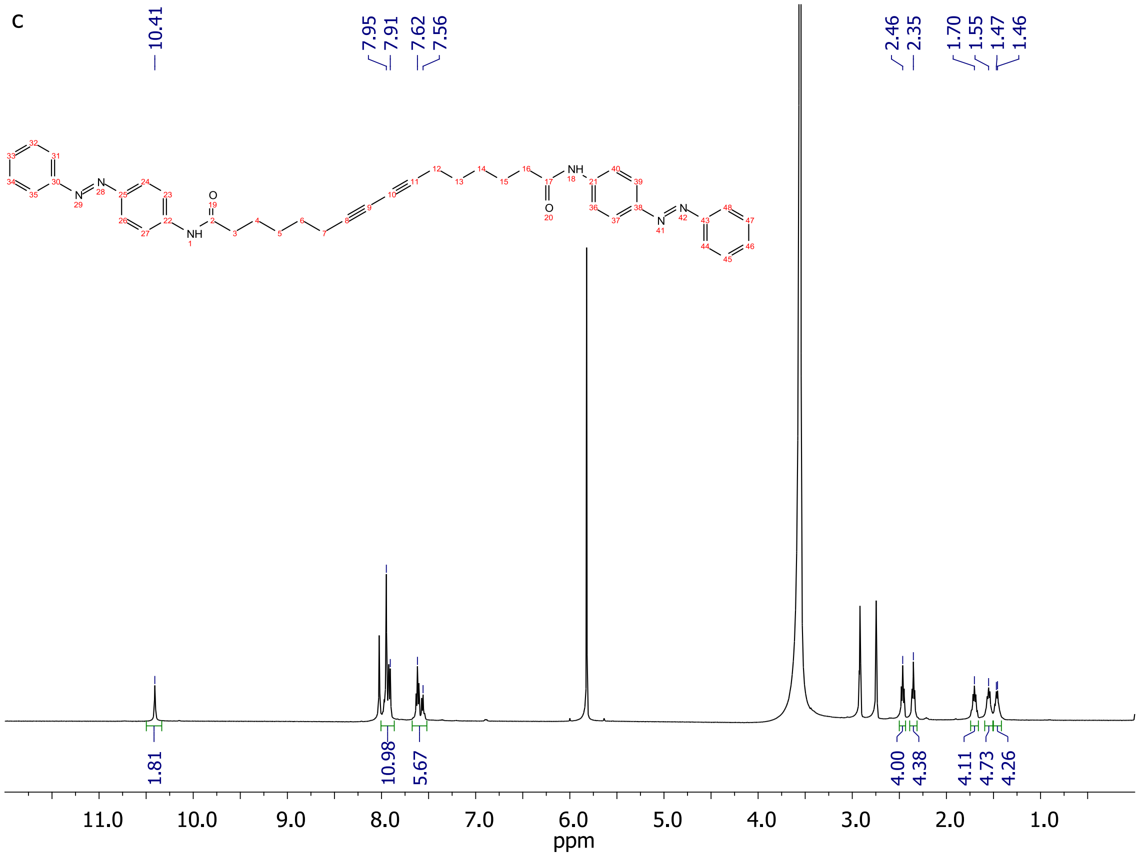
10.41
7.95
7.91
7.62
7.56
2.46
2.35
1.70
1.55
1.47
1.46
NH
O
N
1.81
10.98
5.67
4.00
4.38
4.11
4.73
4.26
11.0
10.0
9.0
8.0
7.0
6.0
5.0
4.0
3.0
2.0
1.0
ppm

d

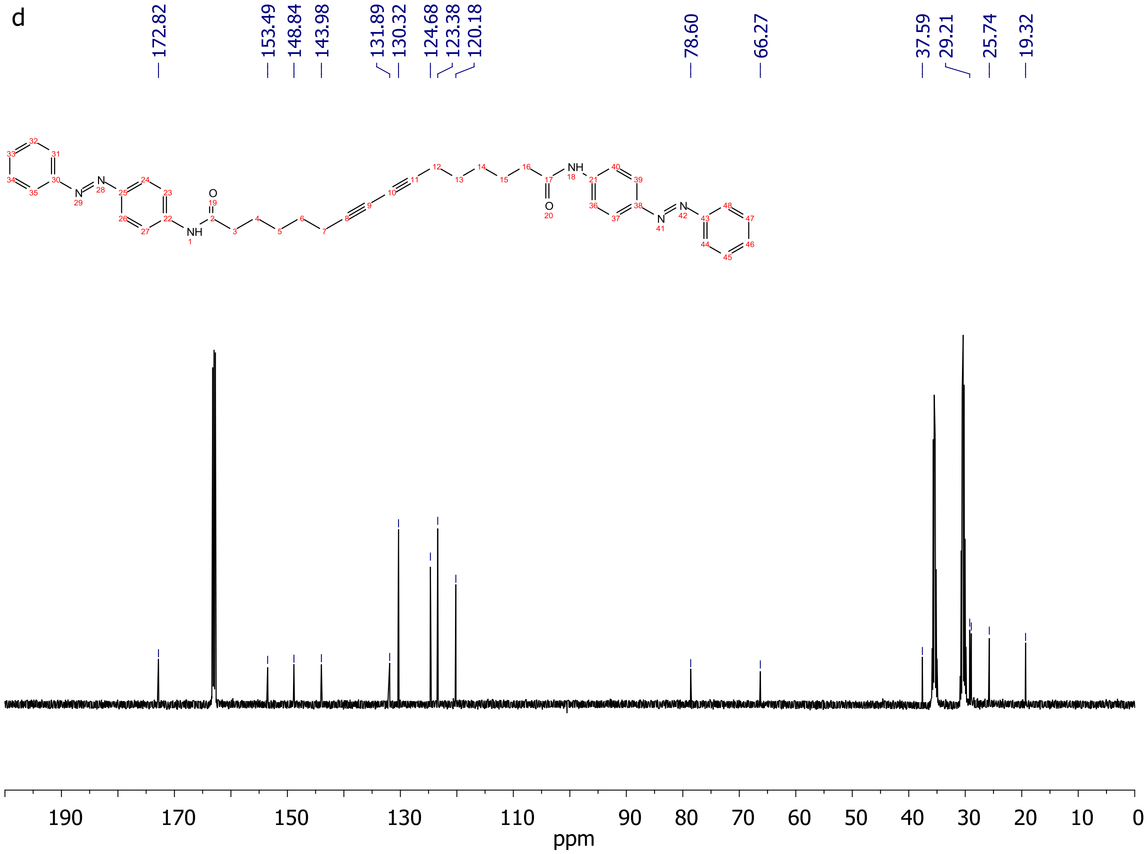
172.82
153.49
148.84
143.98
131.89
130.32
124.68
123.38
120.18
78.60
66.27
37.59
29.21
25.74
19.32
NH
O
N
190
170
150
130
110
90
80
70
60
50
40
30
20
10
0
ppm

e

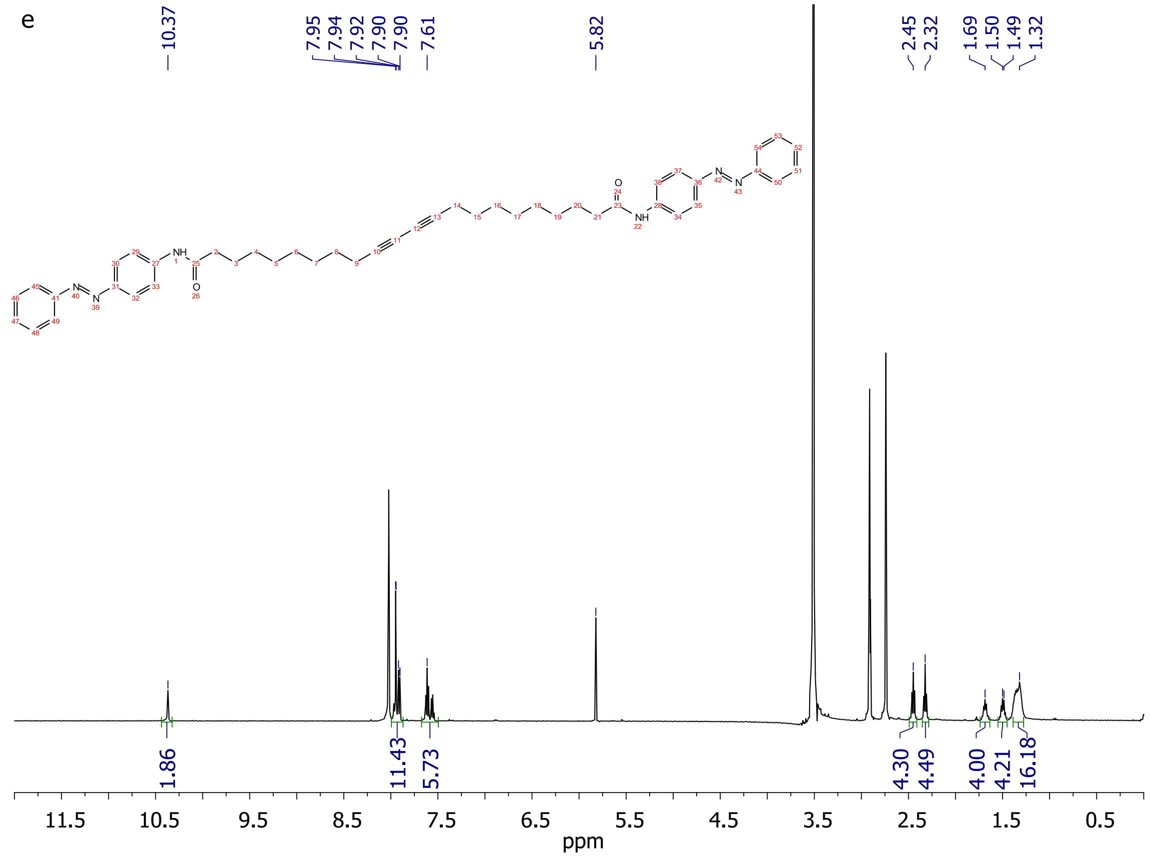

10.37
7.95
7.94
7.92
7.90
7.90
7.61
5.82
2.45
2.32
1.69
1.50
1.49
1.32
NH
O
NH
O
N
N
N
N
1.86
11.43
5.73
4.30
4.49
4.00
4.21
16.18
11.5
10.5
9.5
8.5
7.5
6.5
5.5
4.5
3.5
2.5
1.5
0.5
ppm

f

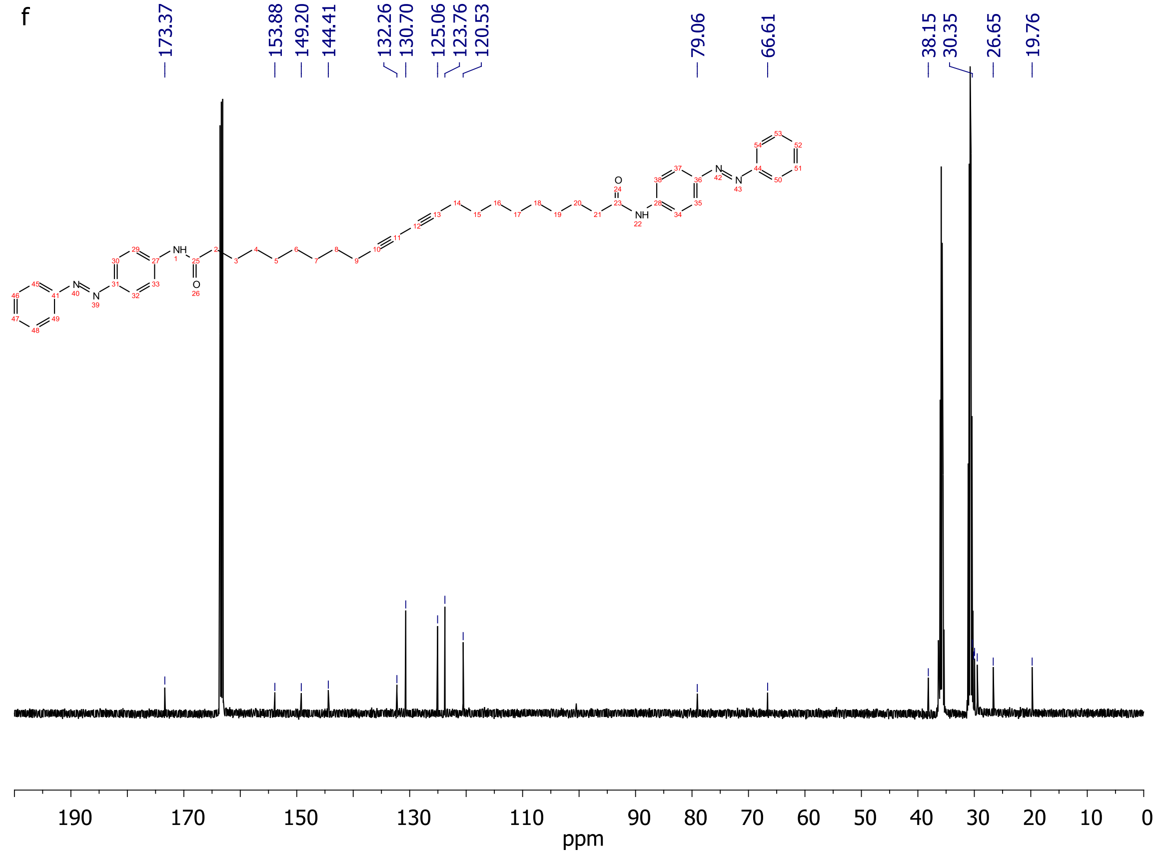

173.37
153.88
149.20
144.41
132.26
130.70
125.06
123.76
120.53
79.06
66.61
38.15
30.35
26.65
19.76
NH
O
NH
O
N
N
N
N
190
170
150
130
110
90
80
70
60
50
40
30
20
10
0
ppm

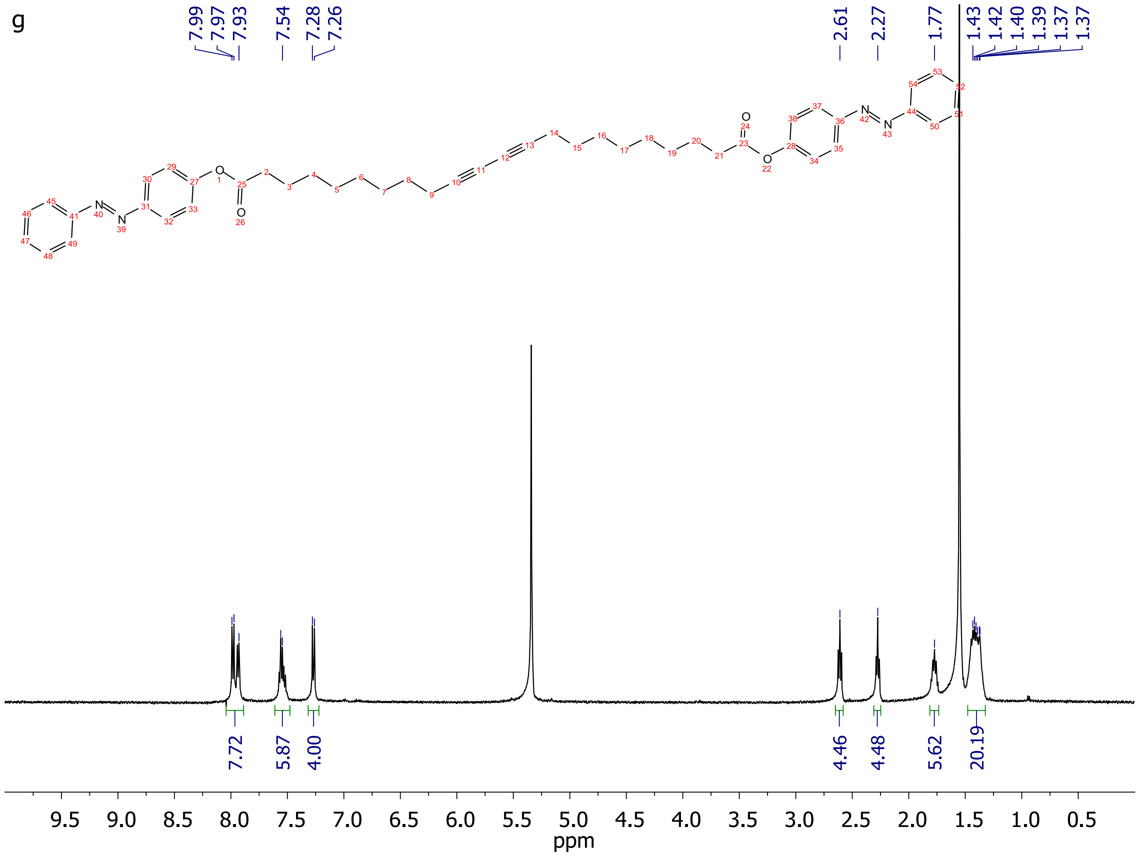
g
7.99
7.97
7.93
7.54
7.28
7.26
2.61
2.27
1.77
1.43
1.42
1.40
1.39
1.37
1.37
7.72
5.87
4.00
4.46
4.48
5.62
20.19
9.5 9.0 8.5 8.0 7.5 7.0 6.5 6.0 5.5 5.0 4.5 4.0 3.5 3.0 2.5 2.0 1.5 1.0 0.5
ppm

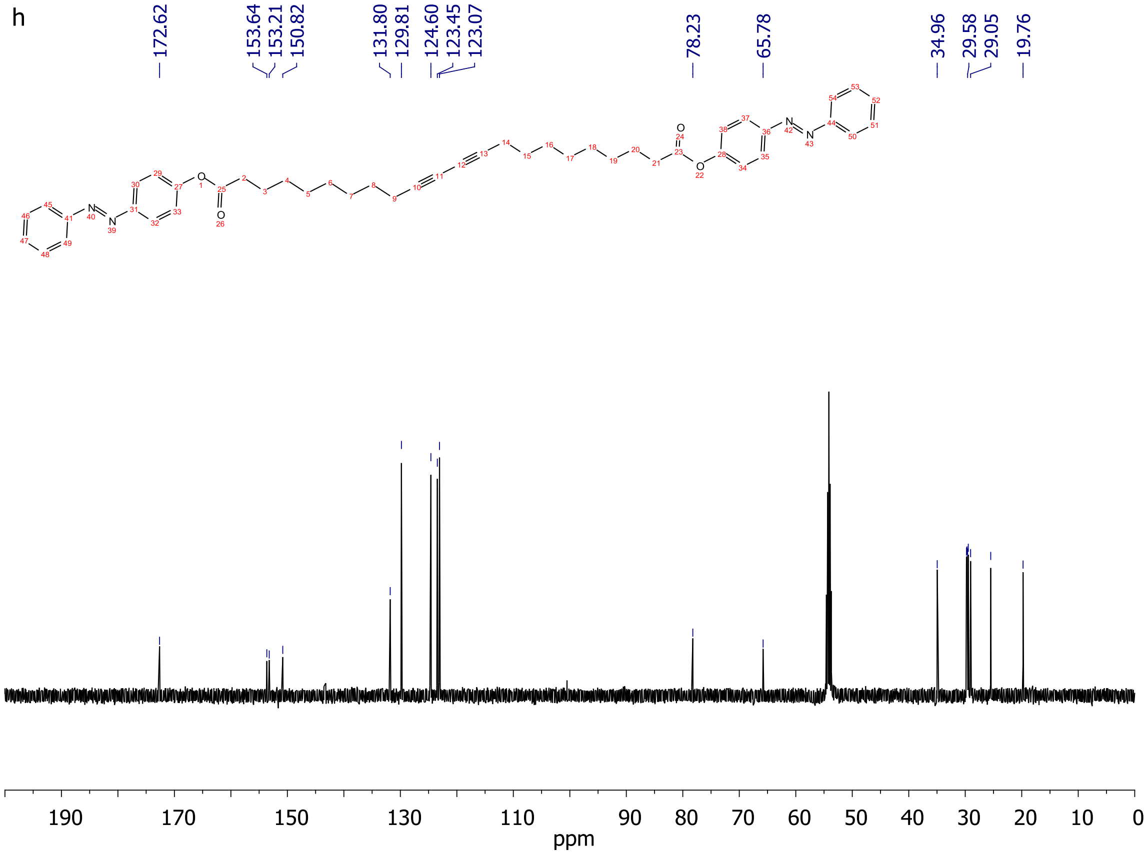
h
172.62
153.64
153.21
150.82
131.80
129.81
124.60
123.45
123.07
78.23
65.78
34.96
29.58
29.05
19.76
190 170 150 130 110 90 80 70 60 50 40 30 20 10 0
ppm

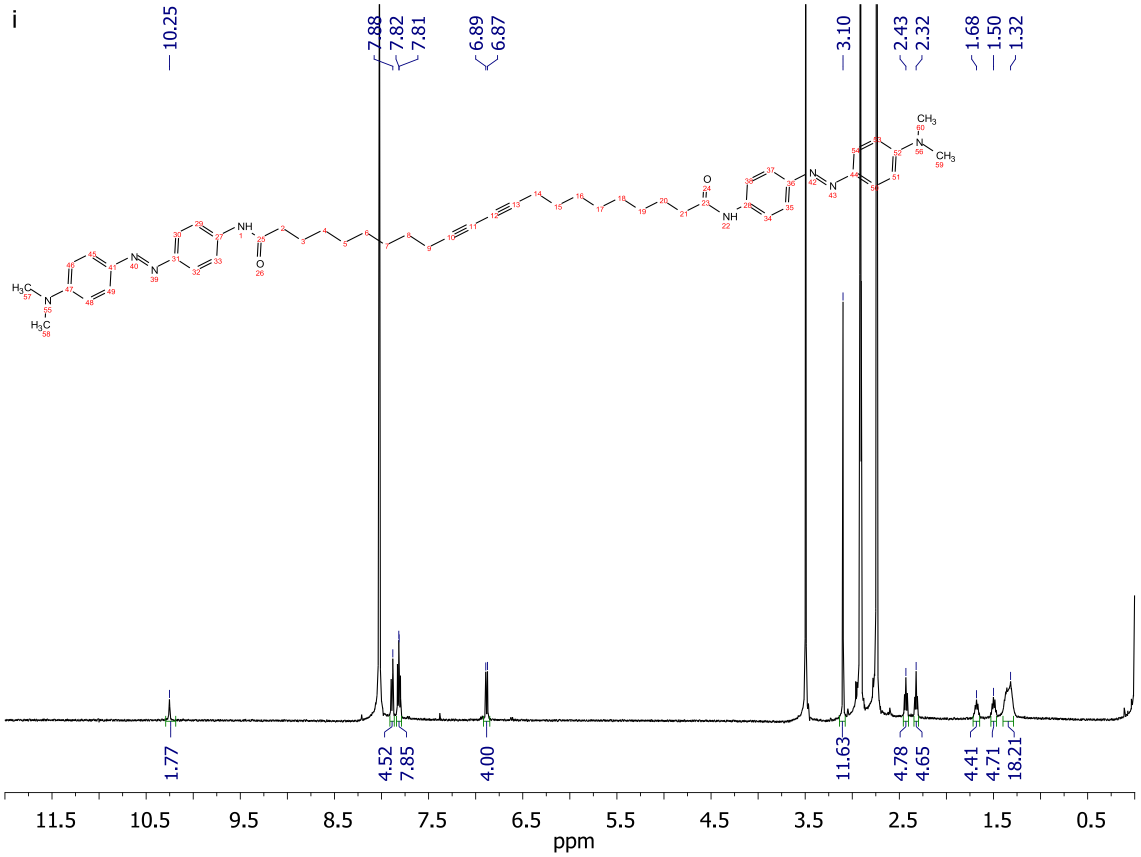
i
10.25
7.88
7.82
7.81
6.89
6.87
3.10
2.43
2.32
1.68
1.50
1.32
1.77
4.52
7.85
4.00
11.63
4.78
4.65
4.41
4.71
18.21
11.5
10.5
9.5
8.5
7.5
6.5
5.5
4.5
3.5
2.5
1.5
0.5
ppm

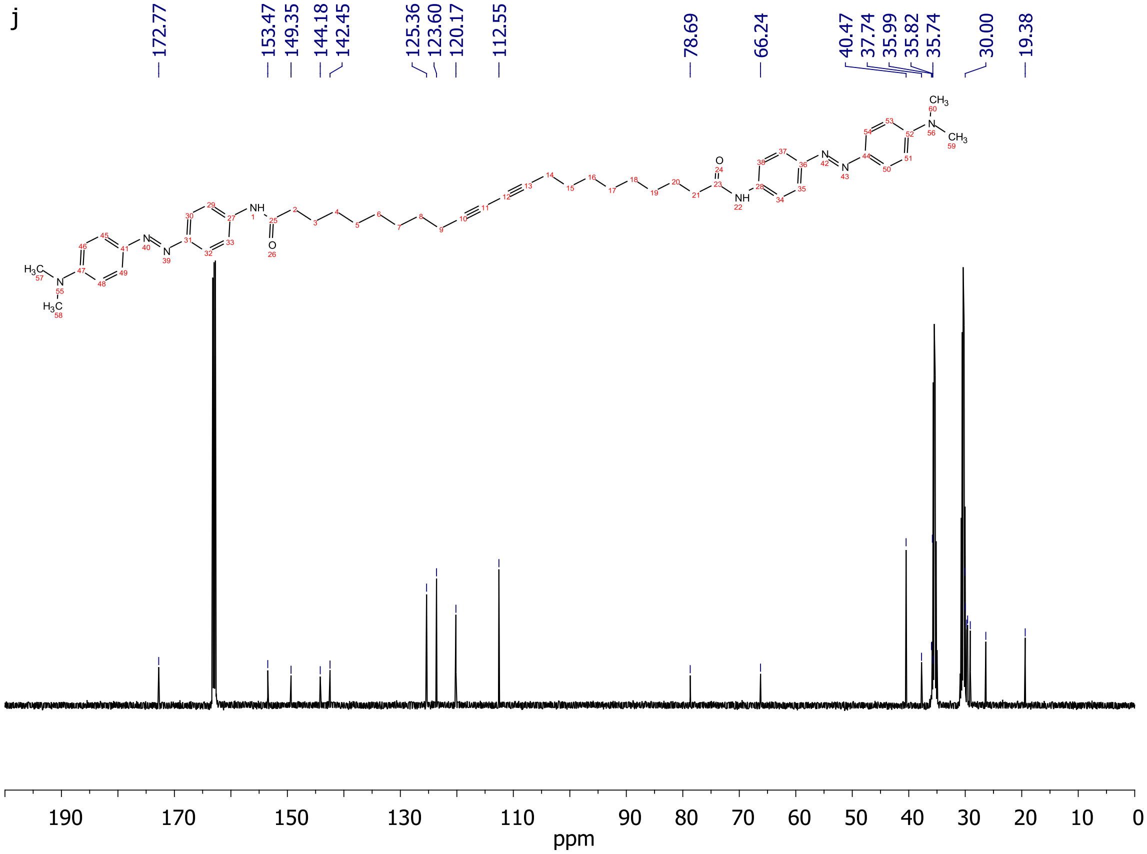
j
172.77
153.47
149.35
144.18
142.45
125.36
123.60
120.17
112.55
78.69
66.24
40.47
37.74
35.99
35.82
35.74
30.00
19.38
190
170
150
130
110
90
80
70
60
50
40
30
20
10
0
ppm

k

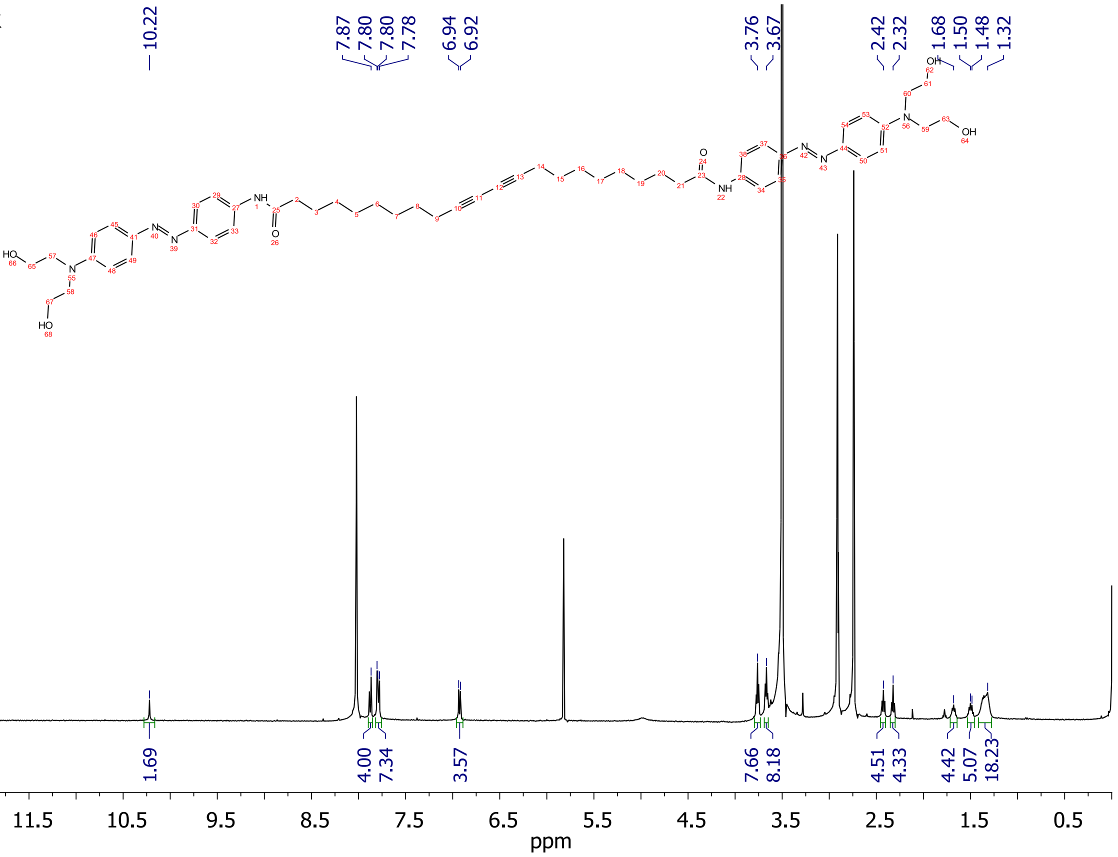

10.22
7.87
7.80
7.80
7.78
6.94
6.92
3.76
3.67
2.42
2.32
1.68
1.50
1.48
1.32
HO
N
OH
NH
O
1.69
4.00
7.34
3.57
7.66
8.18
4.51
4.33
4.42
5.07
18.23
11.5
10.5
9.5
8.5
7.5
6.5
5.5
4.5
3.5
2.5
1.5
0.5
ppm

l

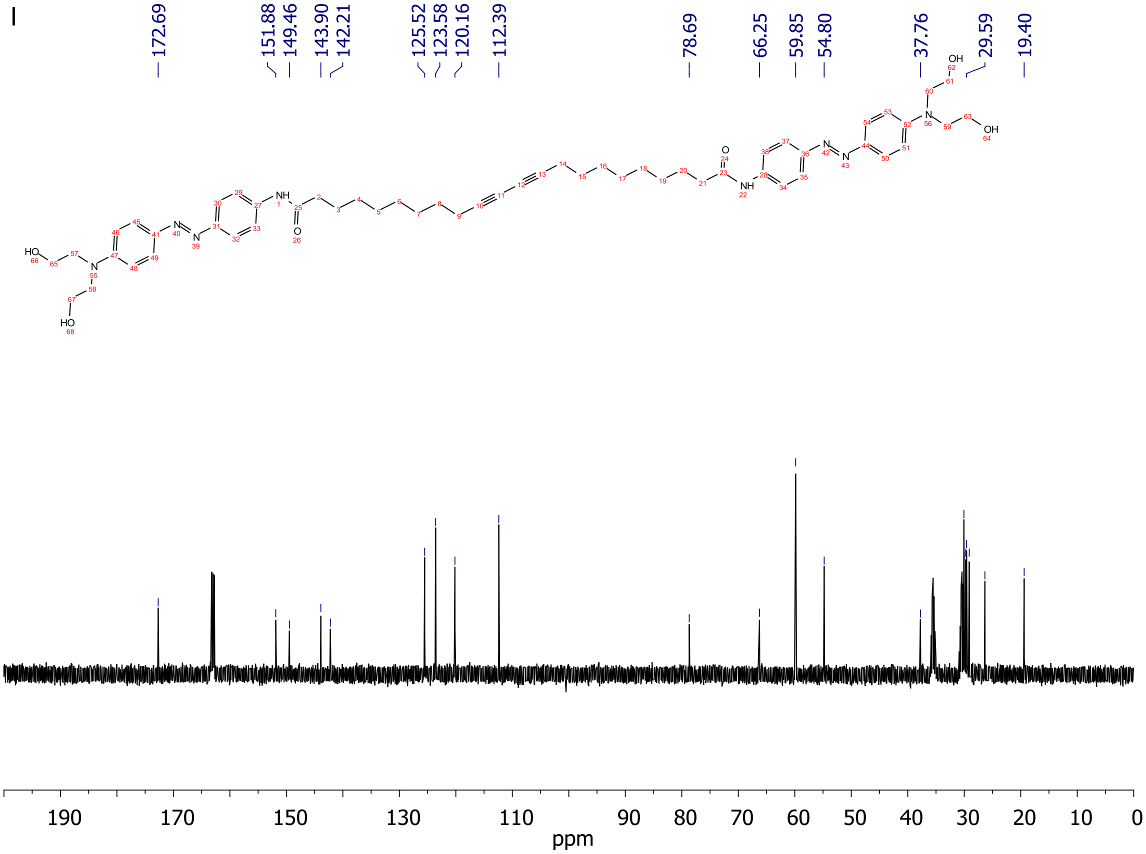

172.69
151.88
149.46
143.90
142.21
125.52
123.58
120.16
112.39
78.69
66.25
59.85
54.80
37.76
29.59
19.40
HO
N
OH
NH
O
190
170
150
130
110
90
80
70
60
50
40
30
20
10
0
ppm

m

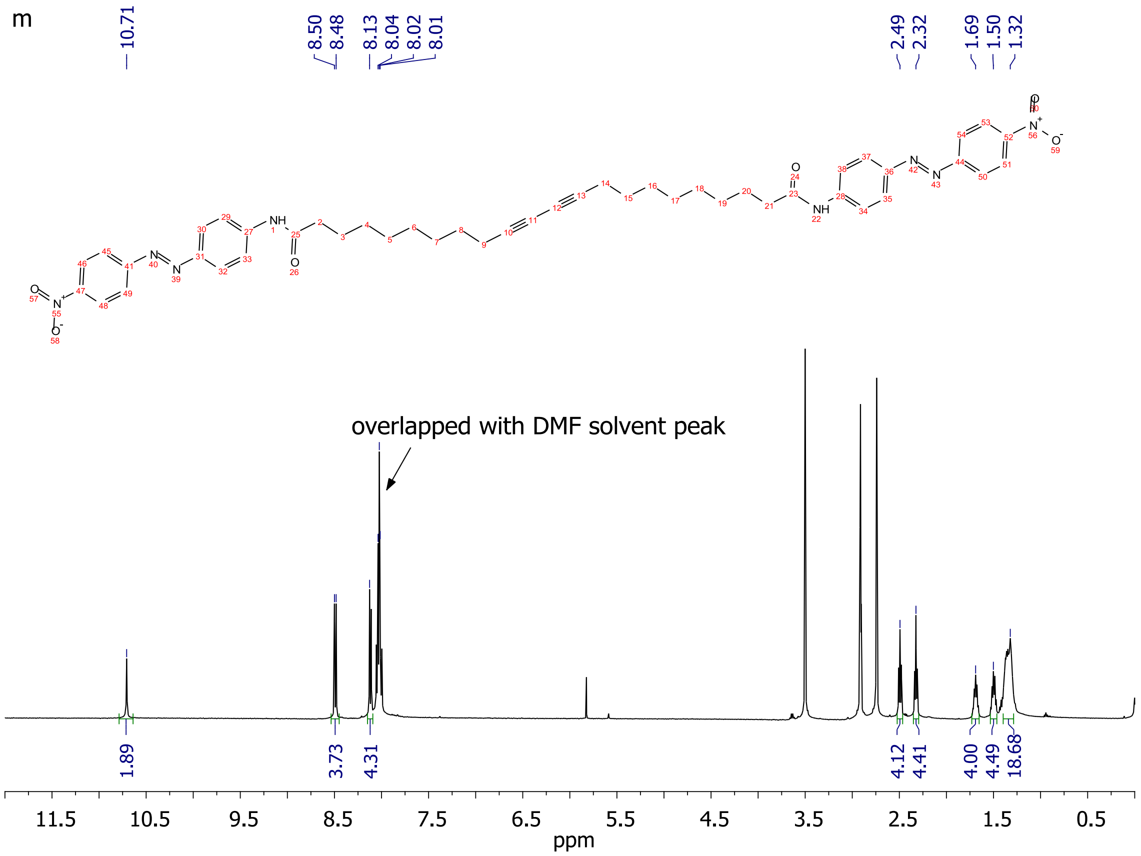
10.71
8.50
8.48
8.13
8.04
8.02
8.01
2.49
2.32
1.69
1.50
1.32
overlapped with DMF solvent peak
1.89
3.73
4.31
4.12
4.41
4.00
4.49
18.68
11.5
10.5
9.5
8.5
7.5
6.5
5.5
4.5
3.5
2.5
1.5
0.5
ppm

n

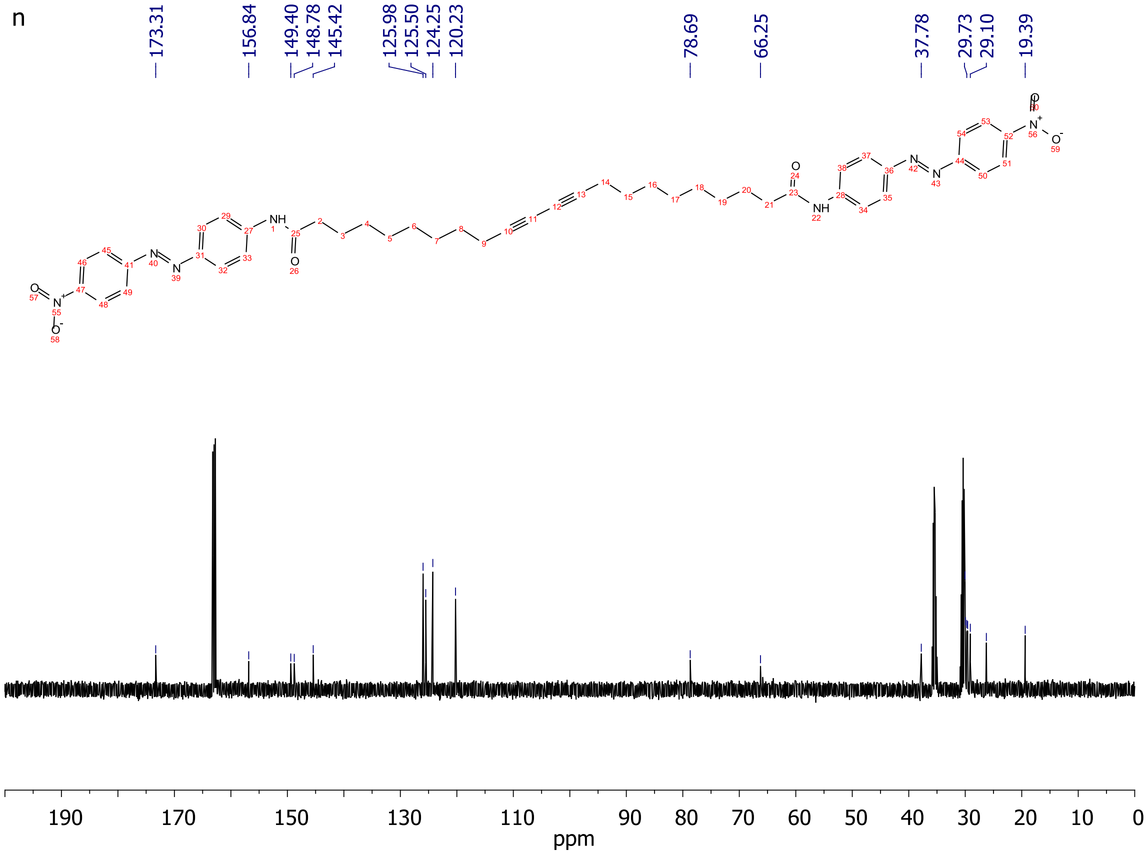
173.31
156.84
149.40
148.78
145.42
125.98
125.50
124.25
120.23
78.69
66.25
37.78
29.73
29.10
19.39
190
170
150
130
110
90
80
70
60
50
40
30
20
10
0
ppm

o

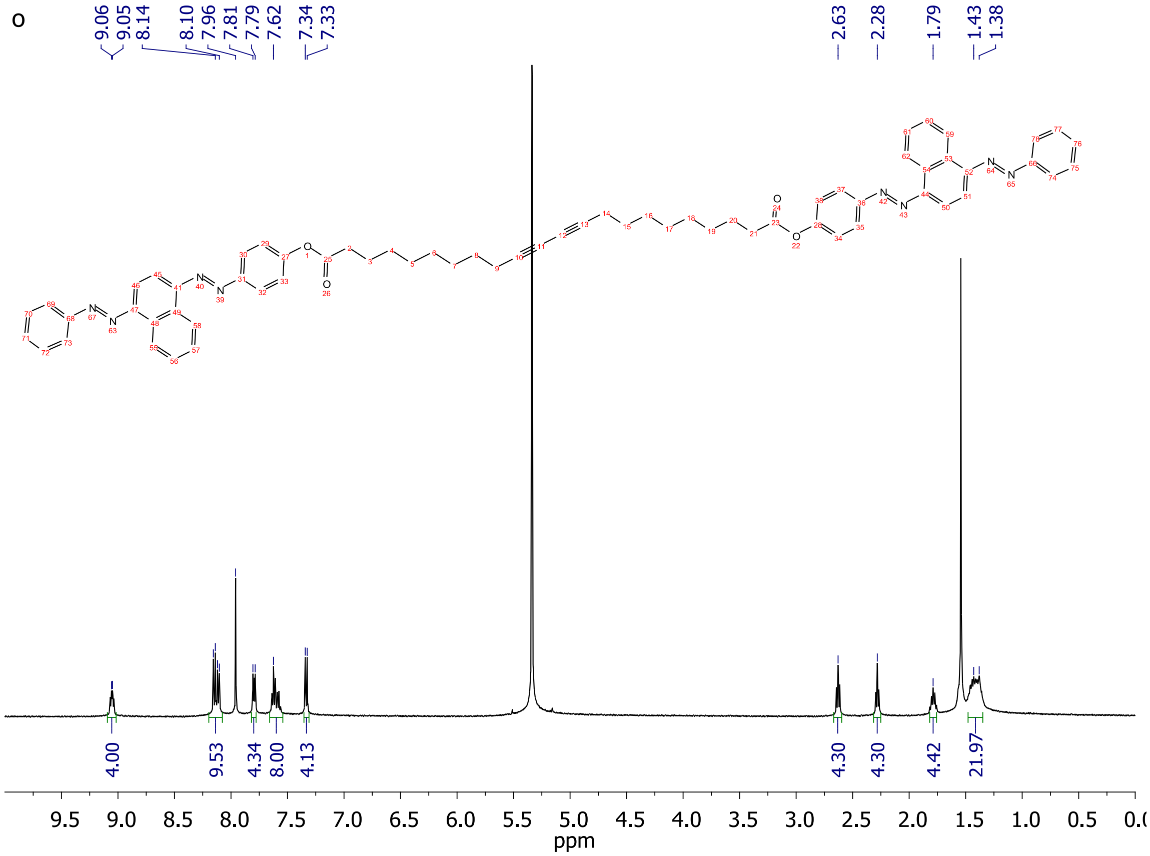
9.06
9.05
8.14
8.10
7.96
7.81
7.79
7.62
7.34
7.33
2.63
2.28
1.79
1.43
1.38
4.00
9.53
4.34
8.00
4.13
4.30
4.30
4.42
21.97
9.5
9.0
8.5
8.0
7.5
7.0
6.5
6.0
5.5
5.0
4.5
4.0
3.5
3.0
2.5
2.0
1.5
1.0
0.5
0.0
ppm

p

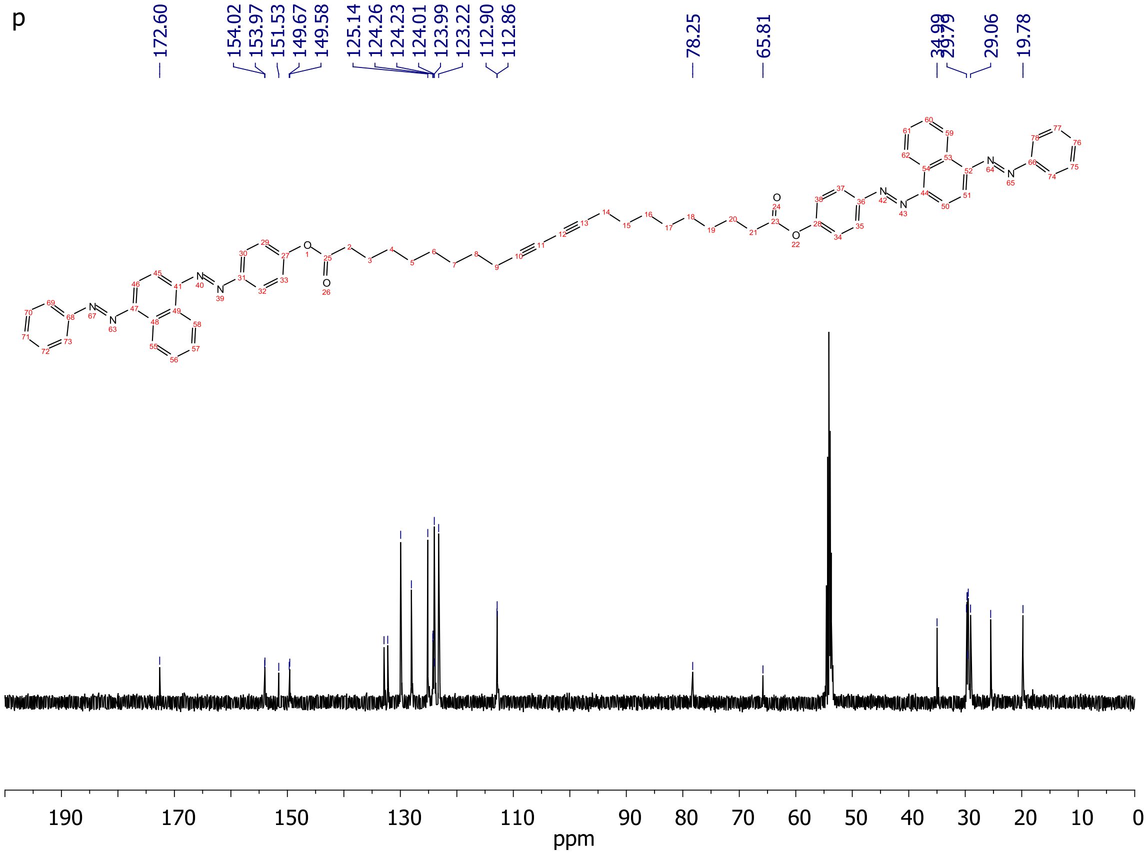
172.60
154.02
153.97
151.53
149.67
149.58
125.14
124.26
124.23
124.01
123.99
123.22
112.90
112.86
78.25
65.81
34.99
29.79
29.06
19.78
190
170
150
130
110
90
80
70
60
50
40
30
20
10
0
ppm

Table S2. X-ray experimental details for compound **3**

Identification code	Compound 3
Empirical formula	$C_{46} H_{52} N_6 O_2$
Formula weight	720.93
Temperature	100(2) K
Wavelength	0.71073 Å
Crystal system	Triclinic
Space group	P -*1*
Unit cell dimensions	a = 5.9062(7) Å
	b = 7.7504(9) Å
	c = 42.123(5) Å
	α = 87.000(2) º
	β = 89.311(2) º
	γ = 86.210(2) º
Volume	1921.3(4) Å^3
Z	2
Density (calculated)	1.246 mg m^{-3}
Absorption coefficient	0.077 mm^{-1}
F(000)	772
Crystal size	0.230 x 0.135 x 0.030 mm^3
θ range for data collection	0.968 to 28.283°
Index ranges	-7<=*h*<=7, -10<=*k*<=9, -56<=*l*<=55
Reflections collected	31218
Independent reflections	8750 [R_{int} = 0.0334]
Absorption correction	Multi-scan
Max. and min. transmission	0.7461 and 0.6528
Refinement method	Full-matrix least-squares on F^2
Data / restraints / parameters	8750 / 2 / 493
Goodness-of-fit[a] on F^2	1.044
R_1[b]	0.0738
wR_2[c]	0.2094

[a] GOF = $(\Sigma\, w(F_o^2 - F_c^2)^2/(n - p))^{1/2}$ where n is the number of data and p is the number of parameters refined. [b] $R_1 = \Sigma\, ||F_o| - |F_c||/\, \Sigma\, |F_o|$. [c] $wR_2 = (\Sigma(w(F_o^2 - F_c^2)^2)/\, \Sigma\, (w(F_o^2)^2))^{1/2}$